



## Heterotrophs are key contributors to nitrous oxide production in mixed liquor under low C-to-N ratios during nitrification - batch experiments and modelling

**Domingo Felez, Carlos; Pellicer i Nàcher, Carles; Petersen, Morten S.; Jensen, Marlene Mark; Plósz, Benedek G.; Smets, Barth F.**

*Published in:*  
Biotechnology and Bioengineering

*Link to article, DOI:*  
[10.1002/bit.26062](https://doi.org/10.1002/bit.26062)

*Publication date:*  
2017

*Document Version*  
Peer reviewed version

[Link back to DTU Orbit](#)

*Citation (APA):*  
Domingo Felez, C., Pellicer i Nàcher, C., Petersen, M. S., Jensen, M. M., Plósz, B. G., & Smets, B. F. (2017). Heterotrophs are key contributors to nitrous oxide production in mixed liquor under low C-to-N ratios during nitrification - batch experiments and modelling. *Biotechnology and Bioengineering*, 114(1), 132-140. <https://doi.org/10.1002/bit.26062>

---

### General rights

Copyright and moral rights for the publications made accessible in the public portal are retained by the authors and/or other copyright owners and it is a condition of accessing publications that users recognise and abide by the legal requirements associated with these rights.

- Users may download and print one copy of any publication from the public portal for the purpose of private study or research.
- You may not further distribute the material or use it for any profit-making activity or commercial gain
- You may freely distribute the URL identifying the publication in the public portal

If you believe that this document breaches copyright please contact us providing details, and we will remove access to the work immediately and investigate your claim.

1 Heterotrophs are key contributors to nitrous oxide production in  
2 mixed liquor under low C-to-N ratios during nitrification – batch  
3 experiments and modelling

4

5

6 **Author list**

7 Carlos Domingo-Félez<sup>1</sup>, Carles Pellicer-Nàcher<sup>1</sup>, Morten S. Petersen<sup>1</sup>, Marlene M.  
8 Jensen<sup>1</sup>, Benedek G. Plósz<sup>1</sup>, Barth F. Smets<sup>1\*</sup>

9

10 <sup>1</sup>Department of Environmental Engineering, Technical University of Denmark, Miljøvej  
11 113, 2800 Kgs. Lyngby, Denmark

12 \* Corresponding author:

13 Barth F. Smets, Phone: +45 4525 1600, Fax: +45 4593 2850, E-mail: [bfsm@env.dtu.dk](mailto:bfsm@env.dtu.dk)

14

15

16

17 Running title: N<sub>2</sub>O production in nitrifying batch experiments: heterotrophic and autotrophic  
18 contributions.

19

20 **Abstract**

21 Nitrous oxide ( $N_2O$ ), a by-product of biological nitrogen removal during wastewater  
22 treatment, is produced by ammonia-oxidizing bacteria (AOB) and heterotrophic  
23 denitrifying bacteria (HB). Mathematical models are used to predict  $N_2O$  emissions,  
24 often including AOB as the main  $N_2O$  producer. Several model structures have been  
25 proposed without consensus calibration procedures. Here, we present a new  
26 experimental design that we used to calibrate AOB-driven  $N_2O$  dynamics of a mixed  
27 culture. Even though AOB activity was favoured with respect to HB, oxygen uptake  
28 rates indicated HB activity. Hence, rigorous experimental design for calibration of  
29 autotrophic  $N_2O$  production from mixed cultures is essential. The proposed  $N_2O$   
30 production pathways were examined using five alternative process models confronted  
31 with experimental data inferred. Individually, the autotrophic and heterotrophic  
32 denitrification pathway could describe the observed data. In the best-fit model, which  
33 combined two denitrification pathways, the heterotrophic contribution to  $N_2O$   
34 production was stronger than the autotrophic. Importantly, the individual contribution of  
35 autotrophic and heterotrophic to the total  $N_2O$  pool could not be unambiguously  
36 elucidated solely based on bulk  $N_2O$  measurements. NO data availability will increase  
37 the practical identifiability of  $N_2O$  production pathways.

38

39 **Keywords:** Nitrous oxide, Batch, Nitrification, Denitrification, Model

40

## 1. Introduction

Nitrous oxide ( $\text{N}_2\text{O}$ ) is known as both a stratospheric ozone depleter and a greenhouse gas with 300 times higher radiative forcing than carbon dioxide (Stocker et al., 2013).

$\text{N}_2\text{O}$  is emitted during biological nitrogen removal and its emission factors are highly variable between wastewater treatment plants (WWTPs) ( $0.01\text{-}3.3\%$   $\text{N}_2\text{O}_{\text{emitted}}/\text{TN}_{\text{removed}}$ ) (Ahn et al., 2010). Moreover, the carbon footprint of a WWTP is highly sensitive to  $\text{N}_2\text{O}$  emissions (Gustavsson and Tumlin, 2013), as an  $\text{N}_2\text{O}$  emission factor of 1% can increase its carbon footprint by 50% (Monteith et al., 2005).

$\text{N}_2\text{O}$  is biologically produced during wastewater treatment by ammonium oxidizing bacteria (AOB) and heterotrophic denitrifying bacteria (HB). AOB can produce  $\text{N}_2\text{O}$  as a by-product of hydroxylamine oxidation ( $\text{NH}_2\text{OH}$ ) or by nitrite ( $\text{NO}_2^-$ ) reduction. As an obligate intermediate during nitrate ( $\text{NO}_3^-$ ) reduction,  $\text{N}_2\text{O}$  can also be produced by HB (Law et al., 2012). The three pathways are commonly known as nitrifier nitrification (NN), nitrifier denitrification (ND) and heterotrophic denitrification (HD), respectively. Certain wastewater constituents such as dissolved oxygen (DO) and  $\text{NO}_2^-$  have been identified as key variables affecting  $\text{N}_2\text{O}$  dynamics (Kampschreur et al., 2009; Schreiber et al., 2012). However, other variables such as inorganic carbon content, known to affect nitrification rates (Jiang et al., 2015; Torà et al., 2010), have shown contradictory results with respect to  $\text{N}_2\text{O}$  (Khunjar et al., 2011; Peng et al., 2015a). Hence, the metabolic regulation of  $\text{N}_2\text{O}$  production is still under study (Perez-Garcia et al., 2014).

Identifying the individual contribution of each pathway is critical for the design of  $\text{N}_2\text{O}$  mitigation strategies.

One way to elaborate on the individual contributions of the pathways is through  $\text{N}_2\text{O}$  process models. Several  $\text{N}_2\text{O}$  models have been proposed for one or two of the aforementioned  $\text{N}_2\text{O}$  production pathways (Guo and Vanrolleghem, 2013; Ni et al.,

66 2013a) with the final goal of mitigating its emissions. Models vary based on the true  
67 substrate considered for AOB ( $\text{NH}_3$  vs.  $\text{NH}_4^+$ ), a reaction's electron donor, or whether  
68 substrate inhibition is considered (Pan et al., 2013; Spérandio et al., 2016). How to  
69 mathematically describe these effects will impact the structural identifiability of model  
70 parameters (Dochain and Vanrolleghem, 2001).

71 Calibration of  $\text{N}_2\text{O}$  models typically rely on the same data series as N-removing models  
72 ( $\text{DO}$ ,  $\text{NH}_4^+$ ,  $\text{NO}_2^-$ ,  $\text{NO}_3^-$ ,  $\text{COD}$ ) and additionally  $\text{N}_2\text{O}$  (Guo and Vanrolleghem, 2013; Ni  
73 et al., 2011). The type and quality of experimental data will affect the practical  
74 identifiability of model parameters (Dochain and Vanrolleghem, 2001). Literature for  
75  $\text{N}_2\text{O}$ -associated parameters shows large variability for similar processes. For example,  
76 the AOB affinity for  $\text{NO}_2^-$  during autotrophic denitrification in nitrifying biomass has  
77 been reported from 0.14 to 8 mgN/L (Kampschreur et al., 2007; Schreiber, 2009).  
78 Similarly, for the same model, a wide range of autotrophic NO affinity constants has  
79 been used, from 0.004 to 1 mgN/L (Mampaey et al., 2013; Spérandio et al., 2016).  
80 Variations can arise from considering different microbial communities, model  
81 assumptions, quality of data or the calibration procedure selected.

82 Depending on the system, AOB or HB have been considered to be the main contributor  
83 to the total  $\text{N}_2\text{O}$  production (Itokawa et al., 2001; Ni et al., 2013a). ND and HD occur  
84 under similar  $\text{DO}$  and  $\text{NO}_2^-$  concentrations, thus leading to possible interferences  
85 between autotrophic and heterotrophic  $\text{N}_2\text{O}$  production (Shen et al., 2015; Wu et al.,  
86 2014). However, under certain operating conditions, the contribution of a pathway can  
87 be considered negligible, thus allowing for more accurate model calibrations.  
88 Experiments can be therefore specifically designed to study the autotrophic contribution  
89 to the total  $\text{N}_2\text{O}$  production pool from mixed liquor biomass. Nitric oxide (NO) is the  
90 direct precursor of  $\text{N}_2\text{O}$  for the three pathways, and even though it is included in most

91 N<sub>2</sub>O models (Ni et al., 2011; Ni et al., 2014) few studies have focused on quantifying  
92 and describing NO emissions (Kampschreur et al., 2007; Schreiber et al., 2009), which  
93 has been shown to be a useful tool to calibrate N<sub>2</sub>O models (Pocquet et al., 2016).

94 In this study, we assess to what extent batch experiments – designed to assess N<sub>2</sub>O  
95 dynamics under nitrifying conditions from a mixed culture biomass from a typical BNR  
96 plant – allow for calibration of N<sub>2</sub>O models. Specifically, without assuming prior  
97 knowledge of the main N<sub>2</sub>O producing pathway, our objective was to:

- 98 ▪ Identify what model structures are capable of describing N<sub>2</sub>O production of mixed  
99 liquor during batch tests at varying substrate concentrations.
- 100 ▪ Quantify the individual contribution of the main biological N<sub>2</sub>O-producing  
101 pathways to the total modelled N<sub>2</sub>O production.
- 102 ▪ Elucidate challenges encountered during calibration of N<sub>2</sub>O models with combined  
103 pathways.

## 104 **2. Materials and Methods**

### 105 **2.1. Batch reactor configuration.**

106 Batch experiments were performed in a 3L PYREX glass vessel (Bellco Glass Inc.,  
107 USA), with 4 side ports used for pH, DO and N<sub>2</sub>O microsensors, and inflow/outflow gas  
108 (Supporting Information (SI), Figure S1). The inlet and outlet gas flow was set at 60  
109 mL/min with gas flow meters. Oxidic and anoxic conditions in the reactor were obtained  
110 by air and N<sub>2</sub> supplied through a bubble diffuser. Aeration and mixing were controlled  
111 using a Labview (National Instruments, Austin, USA) routine. The DO and temperature  
112 data, (CellOx 325, WTW, Germany) and pH (SenTix41, WTW, Germany) was  
113 continuously logged at 0.017 Hz. Liquid N<sub>2</sub>O concentrations were measured with Clark-  
114 type microsensors (N2O-R, Unisense A/S, Aarhus, Denmark). Gaseous N<sub>2</sub>O  
115 concentrations were measured with an infrared gas analyzer (T320, Teledyne, USA).

116 Photometric test kits were used to analyse N-substrates (1.14752, 1.09713, 1.14776,  
117 Merck KGaA, Darmstadt, Germany). Biomass content (MLSS, MLVSS) was measured  
118 in triplicates according to APHA (APHA et al., 1999). Alkalinity was measured by  
119 titration after addition of sulphuric acid (APHA et al., 1999).

## 120 **2.2. Batch tests.**

121 Mixed liquor from a full-scale wastewater treatment plant (Lynetten, Copenhagen,  
122 Denmark) was sampled over a period of three months (May-July 2012). Mixed liquor  
123 was aerated overnight and the biomass concentration adjusted to 2-3 gVSS/L with  
124 aerated clarified wastewater before experiments. After two days of experimentation the  
125 biomass was discarded to prevent significant changes in biomass composition (Torà et  
126 al., 2010). The biomass composition was calculated thermodynamically (SI\_1).  
127 Biomass samples for DNA extraction were taken for every new experiment (n = 8).  
128 Details on the qPCR quantification procedure can be found elsewhere (Terada et al.,  
129 2010) (SI\_2).

130 Two sets of experiments were performed while aeration was kept constant.  
131 Instantaneous extant substrate loadings of 1-3 mgN/gVSS were designed to mimic  
132 typical plant loading conditions, which produce a representative description of the  
133 parent system (Ellis et al., 1996). In the first set of experiments (i) solely  $\text{NH}_4^+$  was  
134 spiked at incremental concentrations (1-8mgN/L).  $\text{NH}_4^+$  removal was monitored off-line  
135 via liquid analysis and online by observing DO drops (Table SII). In the second set of  
136 experiments (ii), again  $\text{NH}_4^+$  spikes (3-5mgN/L) were made and when nearing  $\text{NH}_4^+$   
137 depletion a  $\text{NO}_2^-$  or  $\text{NO}_3^-$  spike (2mgN/L) was made, monitoring responses in liquid and  
138 gas phase. Experiments allowed for nitrogenous concentration changes at both high and  
139 low DO concentrations (DO = 6.5 – 0.2 mg/L), providing useful information regarding  
140 substrate affinities and growth rates and covering a wide range of potential  $\text{N}_2\text{O}$

141 producing scenarios. Experiments were conducted and repeated the day after on  
142 consecutive weeks.

143 Heterotrophic activity was monitored during an anoxic experiment (iii) where  $N_2$  was  
144 supplied instead of air under  $NO_3^-$  excess and no organic carbon addition.  $NO_3^-$   
145 reduction was assumed to occur fed on hydrolysed products originated from biomass  
146 decay as no organic substrate was added. Simultaneously,  $NH_4^+$  would be released and  
147 accumulate in the bulk phase.

148 To determine  $N_2O$  and  $O_2$  mass transfer coefficients, stripping and reoxygenating  
149 experiments (iv) were performed separately at the same batch conditions in preaerated  
150 clarified wastewater (Eq. 1) (Garcia-Ochoa and Gomez, 2009). Liquid phase  $N_2O$   
151 measurements were used to estimate net  $N_2O$  production rates as previously described  
152 (Domingo-Félez et al., 2014) (Eq. 2).

$$153 \quad N_2O_{liq}(t) = N_2O_{liq}(t=0) \cdot e^{(-k_{La}N_2O \cdot t)} \quad (\text{mgN/L}) \quad (\text{Eq. 1})$$

$$154 \quad N_2O \text{ Prod. Rate}_i = \frac{\Delta N_2O_{liq,i}}{\Delta t} + k_{La}N_2O \cdot N_2O_{liq,i} \quad (\text{mgN/L} \cdot \text{min}) \quad (\text{Eq. 2})$$

### 155 **2.3. Model description and calibration: $NH_4^+$ , $NO_2^-$ , $NO_3^-$ , DO.**

156  $NH_4^+$  to  $NO_3^-$  conversion was described by a 2-step nitrification model (Table SIII).  
157 First, AOB oxidize  $NH_4^+$  to  $NH_2OH$  followed by its oxidation to  $NO_2^-$ . Subsequently  
158 NOB oxidize  $NO_2^-$  to  $NO_3^-$ . Heterotrophic denitrification was included as a 4-step  
159 process with  $NO_2^-$ , NO and  $N_2O$  as intermediates (Hiatt and Grady, 2008). Hydrolysis  
160 of particulates and ammonification were simplified into one hydrolytic process  
161 following biomass decay as no particulate N or soluble organic N data was available at  
162 the beginning of the experiments (Table SIV). Rates were not dependent on inorganic  
163 carbon as it was in excess during the experiments (5.8-6.0 mM  $HCO_3^-$ ).



164 The simulation model was implemented in AQUASIM 2.1(Reichert, 1998).  
165 The objective of the following calibration procedure was to fit DO,  $\text{NH}_4^+$ ,  $\text{NO}_2^-$  and  
166  $\text{NO}_3^-$  data. First, physico-chemical parameters ( $k_L a$ ) were estimated from experiments  
167 (iv). Second, nitrification was evaluated by experiments (i) and (ii). The measured  
168  $\text{OUR}_{\text{max}}$  were used to estimate the  $\text{NH}_4^+$  affinity ( $K_{\text{NH}_4}^{\text{AOB}}$ ), and the  $\text{NH}_4^+$  oxidation rates at  
169 varying DO to estimate the DO affinity ( $K_{\text{O}_2, \text{AMO}}^{\text{AOB}}$ ) (SI\_3). Then, oxic hydrolysis was  
170 evaluated against heterotrophic aerobic growth in experiments (i) and (ii) when reduced  
171 nitrogenous species were absent. Anoxic hydrolysis was assessed under anoxic  
172 conditions in experiment (iii). Finally, maximum growth rates ( $\mu_{\text{AOB}}^{\text{AMO}}$ ,  $\mu_{\text{NOB}}$ ) were  
173 estimated from  $\text{NH}_4^+$  removal followed by  $\text{NO}_2^-$  removal and  $\text{NO}_3^-$  accumulation from  
174 experiments (ii). The rest of parameter values describing nitrification and denitrification  
175 were taken from published literature (Table SV). The biomass composition was  
176 modelled throughout the experiments to account for decay processes.

177 After good fits of DO and profiles of  $\text{NH}_4^+$ ,  $\text{NO}_2^-$  and  $\text{NO}_3^-$  were achieved, the  $\text{N}_2\text{O}$   
178 producing model structures (Tables S4) were calibrated.

#### 179 **2.4. Model description and calibration: $\text{N}_2\text{O}$ .**

180 The objective of implementing different  $\text{N}_2\text{O}$  model structures was to investigate what  
181 model structure, with accepted parameters, can describe the experimental data. Two  
182 model structures for AOB driven  $\text{N}_2\text{O}$  production were evaluated. The nitrifier  
183 denitrification (ND) pathway considers the consecutive reduction of  $\text{NO}_2^-$  to NO and  
184  $\text{N}_2\text{O}$  as two processes. The model structure chosen in this study considers DO  
185 inhibition, and  $\text{NH}_2\text{OH}$  is modelled as the electron donor (Ni et al., 2011). The nitrifier  
186 nitrification (NN) pathway considers a 2-step  $\text{NH}_2\text{OH}$  oxidation over NO to  $\text{NO}_2^-$ . A

187 fraction of NO is reduced to N<sub>2</sub>O with NH<sub>2</sub>OH as the electron donor independent of DO  
188 levels (Ni et al., 2013a). Finally, N<sub>2</sub>O can also be produced as an intermediate of  
189 heterotrophic denitrification in the 4-step model (HD) (Hiatt and Grady, 2008). Every  
190 step in the HD pathway considers independently easily biodegradable organic substrate  
191 as electron donor coupled with DO and NO inhibitions. Parameter values from two  
192 different denitrifying activated sludge systems (SRT = 3 and 10 days) (Hiatt and Grady,  
193 2008; Schulthess et al., 1994) have been used regularly to describe HD (Table SVI).  
194 Because the aim of the experiments was to study the autotrophic N<sub>2</sub>O production, both  
195 parameter subsets were considered throughout the study to avoid biases from the  
196 possible heterotrophic contribution: HD\_a and HD\_b.

197 Five different AOB-HB pathway combinations were tested to evaluate what model  
198 structures best describe the experimental N<sub>2</sub>O data (Table I). Three scenarios consider a  
199 single N<sub>2</sub>O production pathway: in scenarios NN and ND only nitrifier nitrification or  
200 nitrifier denitrification produce N<sub>2</sub>O, while HD is modelled as a 2-step denitrification  
201 directly reducing NO<sub>2</sub><sup>-</sup> to N<sub>2</sub> (i.e. no chance of heterotrophic N<sub>2</sub>O production). Scenario  
202 HD considers only N<sub>2</sub>O production through a 4-step denitrification process. Two  
203 scenarios, NN-HD and ND-HD, consider the combination of an autotrophic (either  
204 nitrifying nitrification or denitrification) with the heterotrophic pathway (Ni et al., 2011;  
205 Ni et al., 2013a). Differently from other comparative studies both autotrophic and  
206 heterotrophic pathways are considered without any prior assumption of the main  
207 producer (Spérandio et al., 2016). A multiple-pathway AOB model was not considered  
208 as the assumptions for the ND pathway make it incompatible with the 4-step  
209 denitrification model (Pocquet et al., 2016). The continuity for all the model structures  
210 was numerically evaluated following Hauduc et al. (2010) (Hauduc et al., 2010).

211 For each pathway, only certain parameters are specific to describe N<sub>2</sub>O production. For  
 212 the AOB-associated pathways (NN, ND), only parameters not affecting directly NO<sub>2</sub><sup>-</sup>  
 213 production were first considered:  $\eta_{AOB}$  and  $K_{NO}^{AOB}$  for NN and  $\eta_{AOB}$ ,  $K_{NO}^{AOB}$ ,  $K_{NO_2}^{AOB}$  and  
 214  $K_{i,O_2}^{AOB}$  for ND (Table III). The high number of parameters describing each denitrification  
 215 step (5) does not allow individual parameter estimation. Consequently, a sensitivity  
 216 analysis based on the relative-relative function was used to avoid calibration of  
 217 insensitive parameters in the three pathways. During calibration, the lower and upper  
 218 limits were set to  $\pm 50\%$  from their original literature values.

219 Parameter estimation was performed by minimizing the sum of the squared errors  
 220 weighted by their standard deviations. The likelihood measured of each fit was  
 221 evaluated following Mannina et al. (2011), where an overall model efficiency ( $E_i$ ) value  
 222 of 1 corresponds to a perfect fit and tends zero for large errors (Eq. 3) (Mannina et al.,  
 223 2011), where  $\alpha_j$  corresponds to each data series and  $M_{j,i}$  and  $O_{j,i}$  to modelled and  
 224 observed points.

$$225 \quad E_i = \sum_j^n \alpha_j L(\theta_i/Y_j) = \frac{1}{N} \sum_j^n \alpha_j \cdot \exp\left(-\frac{(\sum(M_{j,i}-O_{j,i})^2)^2}{(\sum(O_{j,i}-\bar{O}_{j,i})^2)^2}\right) \text{ (Eq. 3)}$$

226 In addition, the RMSE was calculated. The contribution of each individual process to  
 227 the N<sub>2</sub>O and NO concentration at any time was calculated by multiplying each process  
 228 rate ( $P_i$ ) with its stoichiometric coefficient ( $v_{ij}$ ). The sum of all terms corresponds to the  
 229 net production/consumption of the state variable ( $S_j$ ) (Eq. 4).

$$230 \quad S_{net\_prod\_j} = \sum_i (P_i \cdot v_{ij}) \quad \text{(Eq. 4)}$$

231 Uncertainty analysis was done following Sin et al. (2010) by randomly sampling  $K_{NO}^{AOB}$   
 232 and  $K_{NO}^{HB}$  ( $0.02 \pm 90\%$  mgN/L).

### 233 **3. Results**

### 234 **3.1.Oxygen uptake and hydrolysis during autotrophic batch experiments.**

235 Experiments (i) and (ii) started with  $\text{NH}_4^+$  and DO excess, reaching first DO followed  
236 by  $\text{NH}_4^+$  limitation. DO reached limiting but never truly anoxic conditions (0.2-0.4 mg  
237 DO/L).  $\text{NO}_2^-$  accumulated shortly and was consumed simultaneously with  $\text{NH}_4^+$  until  
238 depletion, upon which the DO concentration rapidly increased to pre-spike levels.  $\text{NO}_3^-$   
239 accumulated to levels similar to the  $\text{NH}_4^+$  added, indicating complete nitrification of  
240  $\text{NH}_4^+$  (Figure 1, left).

241 Because of the low amount of substrate added a simplified model structure not  
242 including biomass growth was first considered. However, in the absence of  $\text{NH}_4^+$  or  
243  $\text{NO}_2^-$  and at constant aeration DO never reached saturation, indicating an additional  
244 oxygen uptake process (Figure 1, right). Thus the model had to include processes  
245 producing biodegradable carbon from biomass decay. As no other organic source was  
246 present, the heterotrophic aerobic growth was responsible for the continuous oxygen  
247 uptake. Hence, hydrolysis affects DO availability even during short batch tests.

248 Under anoxic conditions hydrolytic processes also release biodegradable carbon and  
249  $\text{NH}_4^+$ . Experimental and modelling results from the anoxic experiment (iii) showed  
250 agreement of ammonification and  $\text{NO}_3^-$  reduction (Figure S2).

### 251 **3.2.N<sub>2</sub>O production during autotrophic batch experiments.**

252 During experiments (i), after  $\text{NH}_4^+$  spikes  $\text{N}_2\text{O}$  increased slowly at high DO and sharply  
253 when reaching  $\text{DO} < 0.5$  mg/L, and decreasing after  $\text{NH}_4^+$  depletion and consequent DO  
254 increase (Figure S3). Experiments (ii) were used to investigate the effect of DO,  
255 followed by  $\text{NO}_2^-$  or  $\text{NO}_3^-$  addition, on  $\text{N}_2\text{O}$  production during  $\text{NH}_4^+$  oxidation. After  
256 adding  $\text{NH}_4^+$ ,  $\text{N}_2\text{O}$  concentration gradually increased until DO became limiting, which

257 rapidly increased its production (Figure 2A, time < 20 min). A  $\text{NO}_3^-$  spike added to  
258 promote heterotrophic denitrification during DO limiting conditions did not increase the  
259 net  $\text{N}_2\text{O}$  production compared to a sole  $\text{NH}_4^+$  spike (Figure 2B). On the other hand,  
260  $\text{NO}_2^-$  addition at low oxygen concentrations and in the presence of  $\text{NH}_4^+$  drastically  
261 increased the  $\text{N}_2\text{O}$  production (Figure 2C). These results are in agreement with literature  
262 where  $\text{NO}_2^-$  showed a larger impact on  $\text{N}_2\text{O}$  production compared to  $\text{NO}_3^-$  under  
263 endogenous conditions (Wu et al., 2014). The net  $\text{N}_2\text{O}$  produced after an  $\text{NH}_4^+$  (or  $\text{NH}_4^+$   
264 followed by  $\text{NO}_3^-$ ) spike was approximately 0.9% of the nitrogen oxidized, while 1.9%  
265 of the nitrogen oxidized was converted to  $\text{N}_2\text{O}$  when  $\text{NH}_4^+$  was spiked followed by  $\text{NO}_2^-$   
266 .

### 267 **3.3. Model calibration for oxygen and nitrogenous substrates.**

268 The objective of the calibration was to obtain a set of parameters that could describe the  
269  $\text{NH}_4^+$ ,  $\text{NO}_2^-$ ,  $\text{NO}_3^-$  and DO profiles before simulating the associated  $\text{N}_2\text{O}$  production.

270 The nitrifying fraction of the mixed liquor was calculated from thermodynamics to be  
271 4.1% AOB and 1.8% NOB of the active biomass (SI\_1). These results are in agreement  
272 with FISH results from other Danish wastewater treatment plants with the same  
273 configuration (AOB = 3-5%, NOB = 2.5-3%) (Mielczarek, 2012). Moreover, 16S  
274 rRNA-based qPCR quantification of dominant AOB and NOB taxa over 11 weeks  
275 showed no variation of the nitrifying community ( $78 \pm 5\%$  AOB/(AOB+NOB), n = 8).

276 NOB affinity constants differ significantly between species (Nowka et al., 2014), thus  
277 NOB affinities were considered as those of *Nitrospira spp.* (Manser et al., 2005)  
278 (*Nitrospira spp.*  $92 \pm 3\%$  relative abundance in comparison to  $8 \pm 3\%$  of *Nitrobacter*  
279 *spp.*). Results from experiments (i) allowed for estimation of the DO affinity for the first

280 nitrification step ( $K_{O_2,AMO}^{AOB} = 0.4$  mg/L), and the  $NH_4^+$  affinity ( $K_{NH_4}^{AOB} = 0.25$  mgN/L)  
281 (Figure S4). The model could describe hydrolysis and ammonification with default  
282 parameter values (Figure S2). Finally, autotrophic maximum specific growth rates  
283 ( $\mu_{AMO}^{AOB}$ ,  $\mu^{NOB}$ ) were estimated with low uncertainty (Table II). After model calibration a  
284 good individual fitting of DO,  $NH_4^+$ ,  $NO_2^-$  and  $NO_3^-$  was obtained ( $R^2 > 0.97$ ,  $n > 30$ )  
285 (Figure 1, left).

### 286 **3.4. Modelling $N_2O$ production from mixed cultures in autotrophic batch tests.**

287 We analysed the capabilities of the model structures considered (NN, ND, HD, NN-HD,  
288 ND-HD) to describe experiments (ii). For each of the five models the best-fit residuals  
289 of the  $N_2O$ -associated parameter subsets are shown in Table III. Results for the models  
290 with the HD\_a parameter subset are described below.

291 **(NN):** *The nitrifying nitrification pathway (NN) describes  $N_2O$  production as a fraction*  
292 *of the oxidized  $NH_4^+$ .* The NN model does not consider an effect of  $NO_2^-$  on the  $N_2O$   
293 produced, and it cannot predict the net  $N_2O$  production increase after  $NO_2^-$  addition  
294 (Figure 2C). The best-fit obtained clearly did not follow the observed  $N_2O$  data (Figure  
295 3) ( $E_{NN} = 0.83$ ).

296 **(ND):** The nitrifying denitrification pathway (ND) could describe the observed  $N_2O$   
297 responses to substrate concentration changes ( $E_{ND} = 0.98$ ). The best-fit parameter subset  
298 increased the  $NO_2^-$  and NO reduction processes with a higher anoxic reduction factor  
299 (Table III). The sensitivity of  $N_2O$  production to  $NO_2^-$  can be described with a low  $NO_2^-$   
300 affinity (Figure 3).

301 **(HD):** Heterotrophic denitrification processes were limited by the organic substrate ( $S_S$ )  
302 and DO inhibited. However, an adequate fit could be obtained ( $E_{HD} = 0.98$ ). Compared

303 to the initial parameter values the NOR process increased its rate compared to NIR and  
304 NOS, indicating a faster NO-to-N<sub>2</sub>O turnover (higher  $\mu_{\text{NOR}}$ ,  $K_{\text{NOR},\text{i},\text{O}_2}^{\text{HB}}$ , lower  $K_{\text{NOR},\text{S}}^{\text{HB}}$ ).

305 **(NN – HD):** *The NN-HD model considered the simultaneous NN and HD associated*  
306 *N<sub>2</sub>O production.* The best fit of the NN-HD model ( $E_{\text{NN-HD}} = 0.97$ ) was obtained when  
307 the NN contribution to the total N<sub>2</sub>O pool was the lowest. This result is in agreement  
308 with the fact that NN-associated N<sub>2</sub>O production could not describe the data while HD-  
309 associated could ( $E_{\text{NN}} = 0.83$  vs.  $E_{\text{HD}} = 0.98$ ). Nonetheless, the best-fit was slightly  
310 worse than the HD model and better than the NN (Figure 3).

311 **(ND – HD):** In the ND-HD model the autotrophic and heterotrophic denitrification  
312 pathways were considered and yielded the best fit ( $E_{\text{ND-HD}} = 0.99$ ). The observed  
313 oxygen-inhibited and NO<sub>2</sub><sup>-</sup>-associated N<sub>2</sub>O production could be best described by two  
314 independent reductive processes.

315 The N<sub>2</sub>O production rates associated to excess DO were much lower, and lasted shorter  
316 periods than N<sub>2</sub>O production under DO-limiting conditions (Figure 2). For this reason,  
317 models containing one or two denitrification pathways (ND, HD, NN-HD, ND-HD)  
318 yielded a better fit than the one associated only with NH<sub>4</sub><sup>+</sup> oxidation (NN). Hence,  
319 models containing at least one denitrification pathway obtained very similar fits but  
320 suggested different N<sub>2</sub>O pathway contributions ( $N_{2\text{O}_{\text{ND}}}$ ,  $N_{2\text{O}_{\text{HD}}} = 0\text{-}100\%$ ) (Figure 3,  
321 Figure S5).

### 322 **3.5. Influence of HD on N<sub>2</sub>O modelling results.**

323 The best N<sub>2</sub>O fit was obtained when two simultaneous denitrification processes were  
324 considered (ND-HD) regardless of the HD parameter subset chosen (Table III, Table  
325 SVII). Even though the total N<sub>2</sub>O production was described equally well by ND-HD\_a

326 and ND-HD\_b, other model outputs showed very different results (Table IV).  
327 Surprisingly, HD was suggested as the main contributor to the total N<sub>2</sub>O pool: 96%  
328 N<sub>2</sub>O<sub>HD\_a</sub>/N<sub>2</sub>O<sub>TOT</sub> and 61% N<sub>2</sub>O<sub>HD\_b</sub>/N<sub>2</sub>O<sub>TOT</sub>. The total NO emitted predicted by the ND-  
329 HD models also showed significant differences (0.2 and 10.5% NO/N<sub>2</sub>O for ND-HD\_a  
330 and ND-HD\_b). Hence, the model could describe the total N<sub>2</sub>O production but neither  
331 the individual N<sub>2</sub>O pathway contribution nor NO emissions.

## 332 **4. Discussion**

### 333 **4.1. Predicting capabilities of N<sub>2</sub>O model structures.**

334 The best-fit obtained for the N<sub>2</sub>O profiles in experiments (ii) varied considerably among  
335 the models considered. However, because of the low N<sub>2</sub>O emission factor, all the N<sub>2</sub>O  
336 models in this study could describe NH<sub>4</sub><sup>+</sup>, NO<sub>2</sub><sup>-</sup>, NO<sub>3</sub><sup>-</sup> and DO profiles.

#### 337 Single pathways

338 In the NN model, N<sub>2</sub>O production is directly linked to NH<sub>2</sub>OH oxidation. The initial  
339 N<sub>2</sub>O production after an NH<sub>4</sub><sup>+</sup> spike can be described by a high concentration of  
340 electron donors and electron acceptors (Figure 2, t < 20 min). Even though the NN  
341 model could not predict the observed N<sub>2</sub>O production at limiting DO and as a response  
342 to NO<sub>2</sub><sup>-</sup> changes (Figure 2C), it was suitable for non-limiting DO conditions (Ni et al.,  
343 2013b; Peng et al., 2015b). The ND model captured the observed N<sub>2</sub>O data, suggesting  
344 complete autotrophic N<sub>2</sub>O production. The larger production of N<sub>2</sub>O at low DO and  
345 high NO<sub>2</sub><sup>-</sup> was captured by changes in oxygen inhibition ( $K_{i,O_2}^{AOB}$ ) and NO<sub>2</sub><sup>-</sup> affinity  
346 ( $K_{NO_2}^{AOB}$ ) from their literature values.

347 Interestingly, the HD model also captured the N<sub>2</sub>O produced suggesting complete  
348 heterotrophic N<sub>2</sub>O production. Even at conditions of minimum C/N and in the presence  
349 of inhibitory DO concentrations for heterotrophic denitrification the best-fit obtained for



350 the ND and HD models were similar ( $E_i = 0.98$ ). It should be highlighted that not  
351 considering hydrolysis, the only carbon source in these experiments, would have  
352 neglected the possible heterotrophic contribution.

### 353 Combined pathways

354 In the NN-HD model, the best-fit results suggest a high HD ( $N_2O_{HD} = 90\%$ ) and small  
355 NN ( $N_2O_{NN} = 10\%$ ) contribution to the total  $N_2O$  pool as the NN pathway is  
356 independent of  $NO_2^-$  levels. Both autotrophic and heterotrophic pathways consider  $N_2O$   
357 production from NO reduction, thus allowing NN-associated  $N_2O$  production to occur  
358 even at low DO regardless of NO's producer. The predictions obtained using the ND-  
359 HD model yielded the best fit ( $E_i > 0.99$ ) by combining two denitrification pathways  
360 and suggested a very low autotrophic contribution ( $N_2O_{ND} = 4\%$ ). Shen et al. (2014)  
361 also suggested that  $N_2O$  production during nitrification could be significantly affected  
362 by the microbial competition with heterotrophic activity (Shen et al., 2015). As two  
363 denitrification processes, ND and HD have similar affinities for N-substrate and DO.  
364 Moreover, the organic carbon limitation of heterotrophs under low C/N is counteracted  
365 by a larger fraction of the microbial community in mixed liquor. ND and HD can  
366 therefore co-occur at similar conditions and rates, which difficult the identifiability of  
367 individual pathways solely with bulk  $N_2O$  measurements.

368 Hence, one cannot ignore heterotrophic contribution to  $N_2O$  even during a short batch  
369 test where the only carbon source was released from hydrolysis of decay products. This  
370 is illustrated by two different combined ND-HD models that could best describe the  
371 observed data with parameter values within literature range.

372 Spérandio *et al.* (2016) compared five  $N_2O$  models (HD + NN or ND) to four long-term  
373 dataseries (Spérandio et al., 2016). The relative contribution of autotrophs (ND) and

374 heterotrophs (HD) to the total N<sub>2</sub>O production was calculated for a full-scale UCT  
375 process. For every 3 units of N<sub>2</sub>O produced by the ND pathway 2 were consumed by  
376 HD, highlighting the importance of including the HD under AOB-driven N<sub>2</sub>O  
377 production.

378 The better performance of multiple-pathway models suggests that new and more  
379 complex models will be necessary to predict N<sub>2</sub>O emissions from dynamic systems  
380 (Spérandio et al., 2016). Considering additional pathways increases their fitting  
381 capabilities but, as highlighted in this study, our understanding of simple models is still  
382 limited. Moreover, overparameterization might compromise the precision and  
383 identifiability of complex models, which has not been critically addressed yet. This will  
384 support the model discrimination procedure towards developing a new biologically  
385 congruent N<sub>2</sub>O model.

#### 386 **4.2.Limitations of modelling combined N<sub>2</sub>O production pathways from bulk** 387 **N<sub>2</sub>O measurements.**

388 The aim of modelling biological N<sub>2</sub>O production during wastewater treatment  
389 operations is to mitigate its emissions by understanding how operating conditions relate  
390 to N<sub>2</sub>O production. The desired mitigation strategies of N<sub>2</sub>O models are specific to the  
391 main producing pathway. If the production of each pathway is accounted for  
392 individually we can better understand the relevant N<sub>2</sub>O producing processes (Ni et al.,  
393 2014). However, because no direct pathway measurements are possible, model  
394 predictions are considered instead. N<sub>2</sub>O models are usually calibrated with N<sub>2</sub>O bulk  
395 measurements (liquid or gas phase), from which the contribution of each pathway is  
396 calculated (Guo and Vanrolleghem, 2013; Ni et al., 2014). The uncertainty associated to

397 model predictions can be calculated by mapping input uncertainty (error in parameter  
398 estimates) onto model outputs.

399 The high variability found in N<sub>2</sub>O model parameters was studied in the ND-HD model  
400 by varying one parameter commonly fixed ( $K_{NO}^{AOB}$ ,  $K_{NO}^{HB}$ ) within literature range (Hiatt  
401 and Grady, 2008; Spérandio et al., 2016). Because the total N<sub>2</sub>O production is not  
402 sensitive to these parameters (data not shown) no effect is seen in the model output for  
403 experiments (ii) (Figure 4, Figure S6). However, variables such as the autotrophic N<sub>2</sub>O  
404 contribution or the total NO production can vary significantly (Figure 4A,B). These  
405 results indicate that fixing  $K_{NO}$  values from literature values can lower model predicting  
406 capabilities for individual N<sub>2</sub>O pathway contributions based on calibrations from N<sub>2</sub>O  
407 bulk measurements.

408 NO plays an important role in N<sub>2</sub>O production as its precursor in every production  
409 pathway (HD, ND, NN) and can, under certain conditions, contribute more than N<sub>2</sub>O to  
410 the nitrogen loss (Castro-Barros et al., 2016). In experiments (ii), measuring NO would  
411 help to elucidate the main NO and N<sub>2</sub>O production pathways by not lumping NO<sub>2</sub><sup>-</sup> and  
412 NO reduction processes, an assumption made by new N<sub>2</sub>O models (Ni et al., 2014;  
413 Pocquet et al., 2016). For a combination of  $K_{NO}^{AOB}$  and  $K_{NO}^{HB}$  values the model output for  
414 NO and N<sub>2</sub>O is shown in Figure 5. The total error of N<sub>2</sub>O production, shown as RMSE,  
415 does not vary regardless of the  $K_{NO}^{AOB}$ - $K_{NO}^{HB}$  values (Figure 5A). On the other hand, both  
416 the contribution of the autotrophic pathway (Figure 5B) and the total NO produced  
417 (Figure 5C) vary significantly (1-56%  $N_2O_{AOB}/N_2O_{TOT}$ , 0.2-4.0% NO/N<sub>2</sub>O). Thus,  
418 because NO is more sensitive to  $K_{NO}$  than N<sub>2</sub>O is, NO data availability will increase the  
419 identifiability of  $K_{NO}^{AOB}$ - $K_{NO}^{HB}$ . Consequently, the contribution of each N<sub>2</sub>O production  
420 pathway can be estimated more accurately. This is in agreement with the suggestion of

421 Spérandio et al. (2016) of using the ratio  $\text{NO}/\text{N}_2\text{O}$  as a parameter for model  
422 discrimination (Spérandio et al., 2016).

## 423 **5. Conclusions**

424 In this work,  $\text{N}_2\text{O}$  production from nitrifying batch experiments with mixed liquor was  
425 studied experimentally and compared to predictions by five model structures. Contrary  
426 to our hypothesis even under very low C/N conditions heterotrophic activity was found  
427 comparable to autotrophic nitrification activity in terms of  $\text{N}_2\text{O}$  production.  
428 Interestingly, process models accounting for heterotrophic and autotrophic  
429 denitrification pathways could describe total  $\text{N}_2\text{O}$  profiles only slightly better than  
430 single-pathway denitrification models. In a conventional N-removing system, where  
431 heterotrophs are more abundant than autotrophs, different combinations of  
432 denitrification  $\text{N}_2\text{O}$ -producing pathways could describe the observed biological  $\text{N}_2\text{O}$   
433 production. Thus, based on  $\text{N}_2\text{O}$  bulk measurements from mixed liquor, models cannot  
434 unambiguously elucidate the contribution of each  $\text{N}_2\text{O}$  production pathway due to  
435 parameter uncertainty.

## 436 **Acknowledgements**

437 This research was funded by the Danish Agency for Science, Technology and  
438 Innovation through the Research Project LaGas (12-132633). The authors have no  
439 conflict to declare.

440

441 **References**

- 442 Ahn JH, Kim S, Park H, Rahm B, Pagilla K, Chandran K. 2010. N<sub>2</sub>O emissions from  
443 activated sludge processes, 2008-2009: results of a national monitoring survey in  
444 the United States. *Environ. Sci. Technol.* **44**:4505–11.
- 445 APHA, AWWA, WEF. 1999. Standard Methods for the Examination of Water and  
446 Wastewater. Ed. American Public Health Association 20th ed. Washington DC.
- 447 Castro-Barros C, Rodríguez-Caballero A, Volcke EIP, Pijuan M. 2016. Effect of nitrite  
448 on the N<sub>2</sub>O and NO production on the nitrification of low-strength ammonium  
449 wastewater. *Chem. Eng. J.* **287**:269–276.
- 450 Dochain D, Vanrolleghem PA. 2001. Dynamic Modelling and Estimation in  
451 Wastewater Treatment Processes. London, UK: IWA Publishing.
- 452 Domingo-Félez C, Mutlu a G, Jensen MM, Smets BF. 2014. Aeration Strategies To  
453 Mitigate Nitrous Oxide Emissions from Single-Stage Nitrification/Anammox  
454 Reactors. *Environ. Sci. Technol.* **48**:8679–8687.
- 455 Ellis TG, Barbeau DS, Smets BF, Grady CPL. 1996. Respirometric technique for  
456 determination of extant kinetic parameters describing biodegradation. *Water  
457 Environ. Res.* **68**:917–926.
- 458 Garcia-Ochoa F, Gomez E. 2009. Bioreactor scale-up and oxygen transfer rate in  
459 microbial processes: an overview. *Biotechnol. Adv.* **27**:153–76.
- 460 Guo L, Vanrolleghem P a. 2013. Calibration and validation of an activated sludge  
461 model for greenhouse gases no. 1 (ASMG1): prediction of temperature-dependent  
462 N<sub>2</sub>O emission dynamics. *Bioprocess Biosyst. Eng.* **1**.
- 463 Gustavsson DJI, Tumlin S. 2013. Carbon footprints of Scandinavian wastewater  
464 treatment plants. *Water Sci. Technol.* **68**:887.
- 465 Hauduc H, Rieger L, Takács I, Héduit A, Vanrolleghem PA, Gillot S. 2010. A  
466 systematic approach for model verification: application on seven published  
467 activated sludge models. *Water Sci. Technol.* **61**:825–39.
- 468 Hiatt WC, Grady CPL. 2008. An updated process model for carbon oxidation,  
469 nitrification, and denitrification. *Water Environ. Res.* **80**:2145–2156.
- 470 Itokawa H, Hanaki K, Matsuo T. 2001. Nitrous oxide production in high-loading  
471 biological nitrogen removal process under low COD/N ratio condition. *Water Res.*  
472 **35**:657–664.
- 473 Jiang D, Khunjar WO, Wett B, Murthy SN, Chandran K. 2015. Characterizing the  
474 Metabolic Trade-Off in *Nitrosomonas europaea* in Response to Changes in  
475 Inorganic Carbon Supply. *Environ. Sci. Technol.* **49**:2523–31.
- 476 Kampschreur MJ, Picioreanu C, Tan N, Kleerebezem R, Jetten MS., van Loosdrecht  
477 MC. 2007. Unraveling the Source of Nitric Oxide Emission During Nitrification.  
478 *Water Environ. Res.* **79**:2499–2509.
- 479 Kampschreur MJ, Temmink H, Kleerebezem R, Jetten MSM, van Loosdrecht MCM.  
480 2009. Nitrous oxide emission during wastewater treatment. *Water Res.* **43**:4093–  
481 103.
- 482 Khunjar WO, Jiang D, Murthy S, Wett B, Chandran K. 2011. Linking the Nitrogen and  
483 One-Carbon Cycles - The Impact of Inorganic Carbon Limitation on Ammonia  
484 Oxidation and Nitrogen Oxide Emission Rates in Ammonia Oxidizing

485 Bacteria:3199–3207.

486 Law Y, Ye L, Pan Y, Yuan Z. 2012. Nitrous oxide emissions from wastewater treatment  
487 processes. *Philos. Trans. R. Soc. Lond. B. Biol. Sci.* **367**:1265–77.

488 Mampaey KE, Beuckels B, Kampschreur MJ, Kleerebezem R, van Loosdrecht MCM,  
489 Volcke EIP. 2013. Modelling nitrous and nitric oxide emissions by autotrophic  
490 ammonia-oxidizing bacteria. *Environ. Technol.* **34**:1555–1566.

491 Mannina G, Cosenza A, Vanrolleghem PA, Viviani G. 2011. A practical protocol for  
492 calibration of nutrient removal wastewater treatment models. *J. Hydroinformatics*  
493 **13**:575.

494 Manser R, Gujer W, Siegrist H. 2005. Consequences of mass transfer effects on the  
495 kinetics of nitrifiers. *Water Res.* **39**:4633–42.

496 Mielczarek AT. 2012. Microbial Communities in Danish Wastewater Treatment Plants  
497 with Nutrient Removal; Aalborg University, Denmark.

498 Monteith HD, Sahely HR, MacLean HL, Bagley DM. 2005. A Rational Procedure for  
499 Estimation of Greenhouse-Gas Emissions from Municipal Wastewater Treatment  
500 Plants. *Water Environ. Res.* **77**:390–403.

501 Ni B-J, Peng L, Law Y, Guo J, Yuan Z. 2014. Modeling of Nitrous Oxide Production  
502 by Autotrophic Ammonia-Oxidizing Bacteria with Multiple Production Pathways.  
503 *Environ. Sci. Technol.* **48**:3916–24.

504 Ni B-J, Rusalleda M, Pellicer-Nàcher C, Smets BF. 2011. Modeling nitrous oxide  
505 production during biological nitrogen removal via nitrification and denitrification:  
506 extensions to the general ASM models. *Environ. Sci. Technol.* **45**:7768–76.

507 Ni B-J, Ye L, Law Y, Byers C, Yuan Z. 2013a. Mathematical modeling of nitrous oxide  
508 (N<sub>2</sub>O) emissions from full-scale wastewater treatment plants. *Environ. Sci.*  
509 *Technol.* **47**:7795–803.

510 Ni B-J, Yuan Z, Chandran K, Vanrolleghem P a., Murthy S. 2013b. Evaluating four  
511 mathematical models for nitrous oxide production by autotrophic ammonia-  
512 oxidizing bacteria. *Biotechnol. Bioeng.* **110**:153–63.

513 Nowka B, Daims H, Spieck E. 2014. Comparative oxidation kinetics of nitrite-oxidizing  
514 bacteria: nitrite availability as key factor for niche differentiation. *Appl. Environ.*  
515 *Microbiol.* **81**:745–753.

516 Pan Y, Ni B, Yuan Z. 2013. Modeling electron competition among nitrogen oxides  
517 reduction and N<sub>2</sub>O accumulation in denitrification. *Environ. Sci. Technol.*  
518 **47**:11083–91.

519 Peng L, Ni B-J, Ye L, Yuan Z. 2015a. N<sub>2</sub>O production by ammonia oxidizing bacteria  
520 in an enriched nitrifying sludge linearly depends on inorganic carbon  
521 concentration. *Water Res.* **74**:58–66.

522 Peng L, Ni B-J, Ye L, Yuan Z. 2015b. Selection of mathematical models for N<sub>2</sub>O  
523 production by ammonia oxidizing bacteria under varying dissolved oxygen and  
524 nitrite concentrations. *Chem. Eng. J.* **281**:661–668.

525 Perez-Garcia O, Villas-Boas SG, Swift S, Chandran K, Singhal N. 2014. Clarifying the  
526 regulation of NO/N<sub>2</sub>O production in *Nitrosomonas europaea* during anoxic-oxic  
527 transition via flux balance analysis of a metabolic network model. *Water Res.*  
528 **60C**:267–277.

- 529 Pocquet M, Wu Z, Queinnec I, Spérandio M. 2016. A two pathway model for N<sub>2</sub>O  
530 emissions by ammonium oxidizing bacteria supported by the NO/N<sub>2</sub>O variation.  
531 *Water Res.* **88**:948–959.
- 532 Reichert P. 1998. AQUASIM 2.0 - User Manual. Computer Program for the  
533 Identification and Simulation of Aquatic Systems. Swiss Federal Institute for  
534 Environmental Science and Technology (EAWAG).
- 535 Schreiber F. 2009. Mechanisms of Transient Nitric Oxide and Nitrous Oxide Production  
536 in a Complex Biofilm\_Sl. *ISME J.*:1–8.
- 537 Schreiber F, Wunderlin P, Udert KM, Wells GF. 2012. Nitric oxide and nitrous oxide  
538 turnover in natural and engineered microbial communities: biological pathways,  
539 chemical reactions, and novel technologies. *Front. Microbiol.* **3**:372.
- 540 Schulthess R Von, Wild D, Gujer W. 1994. Nitric and nitrous oxides from denitrifying  
541 activated sludge at low oxygen concentration. *Water Sci. Technol.* **30**:123–132.
- 542 Shen L, Guan Y, Wu G. 2015. Effect of heterotrophic activities on nitrous oxide  
543 emission during nitrification under different aeration rates. *Desalin. Water Treat.*  
544 **55**:821–827.
- 545 Spérandio M, Pocquet M, Guo L, Ni BJ, Vanrolleghem PA, Yuan Z. 2016. Evaluation  
546 of different nitrous oxide production models with four continuous long-term  
547 wastewater treatment process data series. *Bioprocess Biosyst. Eng.*
- 548 Stocker TF, Qin D, Plattner G-K, Tignor M, Allen SK, Boschung J, Nauels A, Xia Y,  
549 Bex V, Midgley PM. 2013. IPCC Fifth Assessment Report - The physical science  
550 basis. *IPCC*. Cambridge, United Kingdom and New York, NY, USA: Cambridge  
551 University Press 1535 p.
- 552 Terada A, Lackner S, Kristensen K, Smets BF. 2010. Inoculum effects on community  
553 composition and nitrification performance of autotrophic nitrifying biofilm reactors  
554 with counter-diffusion geometry. *Environ. Microbiol.* **12**:2858–2872.
- 555 Torà J a, Lafuente J, Baeza J a, Carrera J. 2010. Combined effect of inorganic carbon  
556 limitation and inhibition by free ammonia and free nitrous acid on ammonia  
557 oxidizing bacteria. *Bioresour. Technol.* **101**:6051–8.
- 558 Wu G, Zhai X, Li B, Jiang C, Guan Y. 2014. Endogenous Nitrous Oxide Emission for  
559 Denitrifiers Acclimated with Different Organic Carbons. *Procedia Environ. Sci.*  
560 **21**:26–32.
- 561

1 Heterotrophs are key contributors to nitrous oxide production in  
2 mixed liquor under low C-to-N ratios during nitrification – batch  
3 experiments and modelling

4  
5

6 **Author list**

7 Carlos Domingo-Félez<sup>1</sup>, Carles Pellicer-Nàcher<sup>1</sup>, Morten S. Petersen<sup>1</sup>, Marlene M.  
8 Jensen<sup>1</sup>, Benedek G. Plósz<sup>1</sup>, Barth F. Smets<sup>1\*</sup>

9

10 <sup>1</sup>Department of Environmental Engineering, Technical University of Denmark, Miljøvej  
11 113, 2800 Kgs. Lyngby, Denmark

12 \* Corresponding author:

13 Barth F. Smets, Phone: +45 4525 1600, Fax: +45 4593 2850, E-mail: [bfsm@env.dtu.dk](mailto:bfsm@env.dtu.dk)

14

15

16

17 Running title: N<sub>2</sub>O production in nitrifying batch experiments: heterotrophic and autotrophic  
18 contributions.

19



20 **List of Figures**

21 **Figure 1** – Left: Concentration profile in a batch experiment after an  $\text{NH}_4^+$  spike  
22 (experimental data: markers, model: lines). Right: Comparison between measured DO  
23 concentrations (diamonds) and model-predicted results when decay and hydrolysis are  
24 considered (black line) or neglected (red line).

25

26 **Figure 2** –  $\text{N}_2\text{O}$  production during batch tests (ii):  $\text{NH}_4^+$  spike (A),  $\text{NH}_4^+$  spike followed  
27 by  $\text{NO}_3^-$  spike (B),  $\text{NH}_4^+$  spike followed by  $\text{NO}_2^-$  spike (C).

28

29 **Figure 3** – Experimental and best-fit simulations of  $\text{N}_2\text{O}$  concentrations during  
30 experiments (i). Individual pathways: HD, ND, NN (left); and combined pathways: ND-  
31 HD, NN-HD (right). Parameter subset HD\_a.

32

33 **Figure 4** – Modelling results for ND-HD\_a best-fit parameters in experiment (ii) (Table  
34 III). 250  $K_{\text{NO}(\text{AOB}, \text{HB})}$  pairs of values sampled randomly in the range  $0.02 \pm 90\%$  mgN/L.  
35 Total contribution (black) and decomposed HD (red) and ND (blue) individual  
36 contributions and to the  $\text{N}_2\text{O}$  pool (left). Total NO production (right). Dashed lines  
37 correspond to the 95% percentiles.

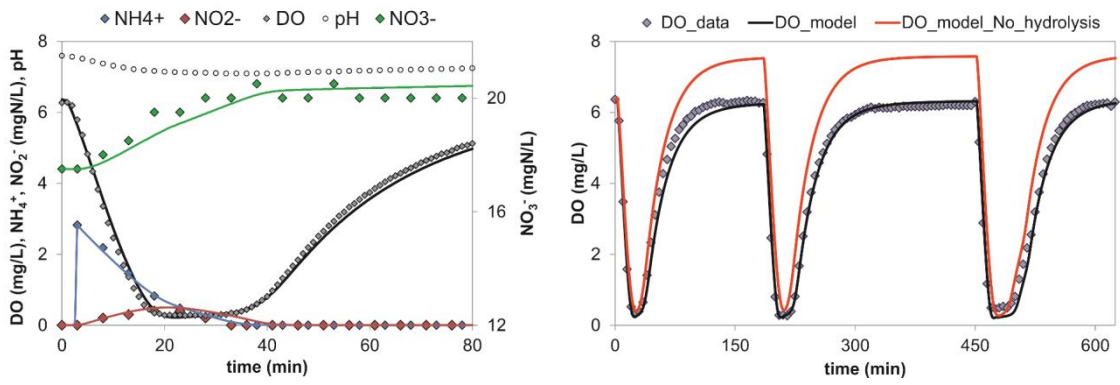
38

39 **Figure 5** – Results of model simulations. Left panels: varying  $K_{\text{NO}}$  values (0.002 – 0.05  
40 mgN/L) for the ND-HD model ( $K_{\text{HB\_NO}}$ ,  $K_{\text{AOB\_NO}}$ ), HD model ( $K_{\text{HB\_NO}}$ ) and ND model  
41 ( $K_{\text{AOB\_NO}}$ ). Right panels: Best-fit results for NN, ND, HD, NN-HD and ND-HD models.  
42 Parameter subset HD\_a.

43 (A)  $\text{N}_2\text{O}$  fit (RMSE), (B) autotrophic contribution to the total  $\text{N}_2\text{O}$  pool, (C)  $\text{NO}/\text{N}_2\text{O}$   
44 produced.

45

46

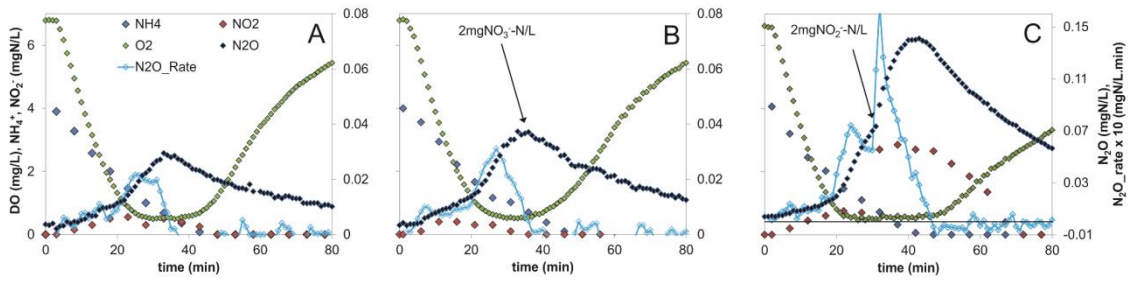


47

48 **Figure 1** – Left: Concentration profile in a batch experiment after an  $\text{NH}_4^+$  spike  
49 (experimental data: markers, model: lines). Right: Comparison between measured DO  
50 concentrations (diamonds) and model-predicted results when decay and hydrolysis are  
51 considered (black line) or neglected (red line).

52

53

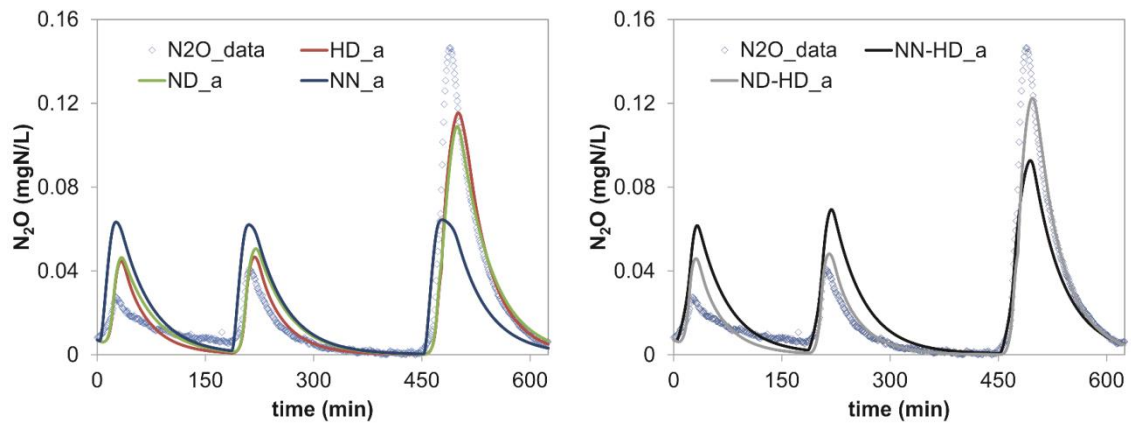


54

55 **Figure 2** – N<sub>2</sub>O production during batch tests (ii): NH<sub>4</sub><sup>+</sup> spike (A), NH<sub>4</sub><sup>+</sup> spike followed  
56 by NO<sub>3</sub><sup>-</sup> spike (B), NH<sub>4</sub><sup>+</sup> spike followed by NO<sub>2</sub><sup>-</sup> spike (C).

57

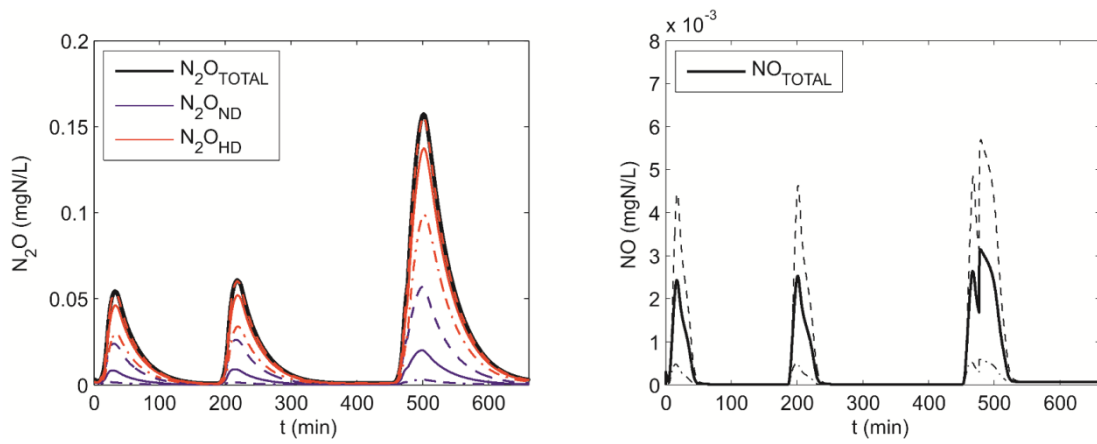
58



59

60 **Figure 3** – Experimental and best-fit simulations of N<sub>2</sub>O concentrations during  
61 experiments (i). Individual pathways: HD, ND, NN (left); and combined pathways: ND-  
62 HD, NN-HD (right). Parameter subset HD\_a.

63

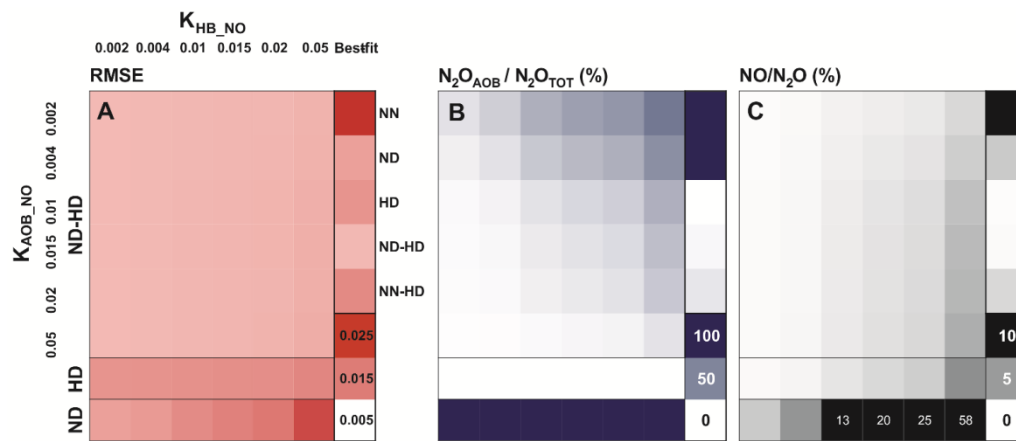


65

66 **Figure 4** – Modelling results for ND-HD\_a best-fit parameters in experiment (ii) (Table  
 67 III). 250  $K_{NO(AOB, HB)}$  pairs of values sampled randomly in the range  $0.02 \pm 90\%$  mgN/L.

68 Total contribution (black) and decomposed HD (red) and ND (blue) individual  
 69 contributions and to the  $N_2O$  pool (left). Total NO production (right). Dashed lines  
 70 correspond to the 95% percentiles.

71



73

74 **Figure 5** – Results of model simulations. Left panels: varying  $K_{NO}$  values (0.002 – 0.05  
 75 mgN/L) for the ND-HD model ( $K_{HB\_NO}$ ,  $K_{AOB\_NO}$ ), HD model ( $K_{HB\_NO}$ ) and ND model  
 76 ( $K_{AOB\_NO}$ ). Right panels: Best-fit results for NN, ND, HD, NN-HD and ND-HD models.

77

Parameter subset HD\_a.

78 (A)  $N_2O$  fit (RMSE), (B) autotrophic contribution to the total  $N_2O$  pool, (C)  $NO/N_2O$   
 79 produced.

80

81

1 Heterotrophs are key contributors to nitrous oxide production in  
2 mixed liquor under low C-to-N ratios during nitrification – batch  
3 experiments and modelling

4  
5

6 **Author list**

7 Carlos Domingo-Félez<sup>1</sup>, Carles Pellicer-Nàcher<sup>1</sup>, Morten S. Petersen<sup>1</sup>, Marlene M.  
8 Jensen<sup>1</sup>, Benedek G. Plósz<sup>1</sup>, Barth F. Smets<sup>1\*</sup>

9

10 <sup>1</sup>Department of Environmental Engineering, Technical University of Denmark, Miljøvej  
11 113, 2800 Kgs. Lyngby, Denmark

12 \* Corresponding author:

13 Barth F. Smets, Phone: +45 4525 1600, Fax: +45 4593 2850, E-mail: [bfsm@env.dtu.dk](mailto:bfsm@env.dtu.dk)

14

15

16

17 Running title: N<sub>2</sub>O production in nitrifying batch experiments: heterotrophic and autotrophic  
18 contributions.

19

20 **Tables**

21 **Table I** – Combination of N<sub>2</sub>O-producing model structures considered.

<b>Scenario</b>	<b>Nitrif. Nitrification</b>	<b>Nitrif. Denitrification</b>	<b>Heter. Denitrification</b>
NN	✓		2 step (no N <sub>2</sub> O)
ND		✓	2 step (no N <sub>2</sub> O)
HD			✓ 4 step ( a / b )
NN-HD	✓		✓ 4 step ( a / b )
ND-HD		✓	✓ 4 step ( a / b )

Heterotrophic denitrification (HD) is modelled with two different parameter subsets (a) and (b).

22

23



24

**Table II** – Best-fit parameter estimates during  $\text{NH}_4^+$ ,  $\text{NO}_2^-$ ,  $\text{NO}_3^-$  and DO

25

**calibration.**

	<b>Initial</b>	<b>Best-fit a</b>	<b>Best-fit b</b>
$\mathbf{u_{AMO} (h^{-1})}$	0.205	$0.182 \pm 0.0019$	$0.187 \pm 0.0023$
$\mathbf{u_{NOB} (h^{-1})}$	0.060	$0.015 \pm 0.0001$	$0.015 \pm 0.0001$
<b>Correlation</b>		0.51	0.55

26

27

**Table III** – Best-fit estimates of N<sub>2</sub>O-related parameters for each model structure considered (HD\_a).

			NN	ND	HD	NN- HD	ND- HD	Lit. Range	Ref.
<b><math>\eta_{AOB}</math></b>	Anoxic reduction factor	(-)	0.28	0.56		0.06	0.56	0.053 - 0.5	(1) (2) (3) (4)
<b><math>K_{AOB NO_2}</math></b>	NO <sub>2</sub> <sup>-</sup> affinity coefficient for denitrification	(mgN/L)		0.61			0.8*	0.14 - 8	(5) (6) (7) (8)
<b><math>K_{AOB i O_2}</math></b>	O <sub>2</sub> inhibition coefficient for denitrification	(mgCOD/L)		0.15			0.15	0.112	(1) (2) (3) (4)
<b><math>u_{NIR}</math></b>	Max. NO <sub>2</sub> <sup>-</sup> reduction rate	(h <sup>-1</sup> )			0.055	0.098	0.059	0.017 - 0.078	(3) (9) (10) (11)
<b><math>u_{NOR}</math></b>	Max. NO reduction rate	(h <sup>-1</sup> )			0.213	0.213	0.137	0.038 - 0.345	(1) (3) (10) (11)
<b><math>u_{NOS}</math></b>	Max. N <sub>2</sub> O reduction rate	(h <sup>-1</sup> )			0.077	0.079	0.125	0.065 - 0.182	(3) (9) (10) (11)
<b><math>K_{HB i O_2 NIR}</math></b>	O <sub>2</sub> inhibition coefficient for NO <sub>2</sub> <sup>-</sup> denitrification	(mgCOD/L)			0.05	0.13	0.05	0.1 - 1	(9) (10) (11)
<b><math>K_{HB i O_2 NOR}</math></b>	O <sub>2</sub> inhibition coefficient for NO denitrification	(mgCOD/L)			0.10	0.03	0.10	0.067 - 1	(1) (3) (10) (11)
<b><math>K_{HB i O_2 NOS}</math></b>	O <sub>2</sub> inhibition coefficient for N <sub>2</sub> O denitrification	(mgCOD/L)			0.03	0.05	0.02	0.031 - 1	(9) (10) (11)
<b><math>K_{HB S NIR}</math></b>	S <sub>s</sub> affinity coefficient for NO <sub>2</sub> <sup>-</sup> denitrification	(mgCOD/L)			0.8	0.8	1.8	1.5 - 20	(9) (10) (11)
<b><math>K_{HB S NOR}</math></b>	S <sub>s</sub> affinity coefficient for NO denitrification	(mgCOD/L)			1.2	1.2	1.2	0.56 - 20	(1) (3) (10) (11)
<b><math>K_{HB S NOS}</math></b>	S <sub>s</sub> affinity coefficient for N <sub>2</sub> O denitrification	(mgCOD/L)			3.0	3.0	3.0	2 - 40	(9) (10) (11)
<b>Best-fit</b>	<b>E<sub>N2O</sub></b>		0.83	0.98	0.98	0.97	0.99		
	<b>RMSE</b>		0.022	0.012	0.013	0.014	0.010		

(1) - Ni *et al.* 2011, (2) - Ni *et al.* 2013a, (3) Ni *et al.* 2013b, (4) Spérandio *et al.* 2016, (5) Schreiber *et al.* 2009, (6) Kampschreur *et al.* 2008, (7) Mampaey *et al.* 2013, (8) Garnier *et al.* 2007,

(9) von Schulthess *et al.* 1994, (10) Guo *et al.* 2013, (11) Hiatt and Grady 2008. \* Fixed value

31

32

**Table IV** – Modelling results for the ND-HD model.

		ND-HD_a	ND-HD_b
$E_i$	(-)	0.993	0.995
$N_2O_{AOB}/TOT$	(%)	4	39
$NO/N_2O$	(%)	0.2	10.5
$NO_{AOB}/TOT$	(%)	67	37
$N_2$	(mgN/L)	0.19	0.39

33

34